Electrocatalysis (2015) 6:493–497
DOI 10.1007/s12678-015-0276-8

LETTER

Overlayer Au-on-W Near-Surface Alloy for the Selective Electrochemical Reduction of CO_2 to Methanol: Empirical (DEMS) Corroboration of a Computational (DFT) Prediction

Alnald Javier[1] · **Jack H. Baricuatro**[1] · **Youn-Geun Kim**[1] · **Manuel P. Soriaga**[1,2]

Published online: 27 August 2015

Introduction

It is now widely known from extensive studies [1–3] over the past few decades on the heterogeneous electrochemical reduction of carbon dioxide in aqueous solutions that, across the vast landscape of CO_2-reduction electrocatalysts, copper stands alone as the single metal that can deliver a remarkable variety of products; unpredictably, however, the product distribution does not include methanol [1–5]. The overall energy conversion efficiency of Cu, defined [6] as the ratio of the free energy of the products generated and that consumed in the electrochemical reduction, is only 30 to 40 %, and the overpotential of Cu at benchmark current densities remains unacceptably large, ca. −1.4 V [1, 6]. The diversity of the product distribution also becomes a major hurdle if only one product is coveted. The desire for catalysts that can perform better than Cu, especially in the generation of methanol, a liquid transportation fuel, and feedstock for direct fuel cells, is thus understandable.

Experimentally, the search for alternative electrocatalysts for CO_2 reduction (CO_2R) has gained only minimal headway because of a lack of fundamental principles on the selective reduction of CO_2 towards a particular product. It had earlier been surmised that the emergence of Cu as the preeminent catalyst for the reduction of CO_2 to compounds more complex than CO and formic acid was due to just the right proportion of the adsorption strengths of carbon monoxide and hydrogen [7–9]: If CO were adsorbed strongly, reactions subsequent to the initial CO_2-to-CO reduction would not occur; if adsorption were weak, or if the adsorption of hydrogen were strong, further reduction of CO would likewise not transpire. Theoretical constructs of volcano or Sabatier plots [7], such as that for the CO_2-to-CH_4 reaction based on $\Delta G°_{CO,ads}$ and $\Delta G°_{H,ads}$ descriptors, invariably resulted in Cu at the top, with metals that had high affinity for CO posted on the left of the volcano and elements that only weakly attract CO placed on the right [7, 9]. Part of the quandary is that, while metals on the left of the volcano plot could be combined with those on the right, the alloy formed would only mimic, but not dramatically improve on, the catalytic properties of pure Cu. Another perplexity is that any fusion of Cu with catalytically inferior metals would only serve to degrade, not enhance, the catalytic capabilities of copper. However, such notions are largely qualitative; a much closer alliance between theory and experiment may yet ferret out quantitative nuances that could lead to unanticipated advances in the catalyst search-and-development mission.

A broadly adopted computational approach in the study of CO_2R catalysts is based on the use of density functional theory (DFT) and substrate-adsorbate interaction energies as descriptors [7, 8, 10]. A recent computational work tackled the selective generation of methanol. The investigation considered three descriptors: one, the adsorption energy of CO, supposedly determines catalytic activity; the other two, the respective adsorption energies of H and OH, ostensibly dictate the selectivity. Bimetallic near-surface alloys (NSA) were selected as materials of interest because, via the methodical combination of the metals to be alloyed, a near-continuous range of interaction energies can be established from which the alloy couple with the most favorable descriptors is identified. The particular NSA that the computational work

✉ Manuel P. Soriaga
soriaga@mail.chem.tamu.edu

[1] Joint Center for Artificial Photosynthesis, California Institute of Technology, Pasadena, CA 91125, USA

[2] Department of Chemistry, Texas A&M University, College Station, TX 77843, USA

converged on is a sub-surface alloy composed of a Au(211) host substrate covered with a monolayer of W that, in turn, is cloaked by a single layer of Au; the latter two monolayers constitute the near-surface alloy. This structure is designated here as Au(211)-[(1×1)-W]-[(1×1)-Au]. The theoretical prediction was that this ideal NSA would show heightened catalytic activity, decreased overpotential, suppressed hydrogen evolution, and preferential production of CH_3OH [9].

The purpose of the present study was the empirical corroboration, via differential electrochemical mass spectrometry (DEMS), of the computational prognostications. The analogue NSA studied was an overlayer of *n* monolayers (ML) of Au on polycrystalline W, denoted as W(pc)-*n*[(1×1)-Au]. It may be noted that the atomic radius of Au, 144 pm, is identical to that of W [11], although Au is face-centered and W is body-centered. The schematic structures of the theoretical and empirical near-surface alloys are depicted in Fig. 1. The test NSA, a Au-on-W bilayer, deviates from the theoretical model in that the host substrate is W and not Au. The viability of W(pc)-(1×1)-Au as a mimic of Au(211)-[(1×1)-W]-[(1×1)-Au] rests on the view that the second sub-surface monolayer only minimally influences the composite interfacial properties of the topmost bilayer.

Experimental

Overlayer Near-Surface Alloy Preparation

There are two types of bimetallic near-surface alloys that consist of discrete layers, as opposed to randomly distributed atoms, of the mixed metals [12–14]: overlayer, in which a single layer of one metal covers the top of another metal, and sub-surface, where the monolayer of the guest metal is located as the second sheet between a single topmost layer and the bulk of the host metal. For convenience in the present introductory study, only the overlayer NSA was considered; if warranted, further work would center on sub-surface alloys.

Electrodeposition of Au-on-W Overlayer A tungsten disk, 1.0 cm in diameter, 0.10 mm thick, and 99.95 % pure, was pared from a W sheet (MTI Corporation, Richmond, CA) and used as the working electrode for the preparation of a Au-on-W near-surface alloy. The W electrode was first immersed in 0.1 M NaOH at 70 °C for at least 3 min to dissolve all surface oxides [15, 16]. After a thorough rinse with Nanopure® water (ThermoFisher Scientific, Waltham, MA), the W electrode was transferred to a 50-mL round-bottom flask with four angled necks (Chemglass, Vineland, NJ) that separately accommodated the working electrode, the 99.9975 %-pure Au counter electrode (Alfa Aesar, Ward Hill, MA), HgO/Hg (1 M NaOH) reference electrode (CH Instruments, Austin, TX), and the N_2-gas inlet line. The precursor solution for Au electrodeposition contained 1.0 mM $AuCl_3$, 99.999 % purity (Sigma-Aldrich, St. Louis, MO), with 0.10 M Na_2CO_3, 99.5 % purity (Macron Chemicals, Central Valley, PA), as supporting electrolyte; the native pH of the solution was 11. The solution was bubbled with N_2 for at least 10 min, prior to potentiostatic deposition at −0.48 V. The open-circuit potential of the W electrode in the precursor solution, under a blanket of N_2, was −0.34 V. The Au coverage was controlled via the deposition time needed to deliver a charge of 0.85 mC cm^{-2}, the equivalent of 1 monolayer (ML) of Au per unit area (cm^2) of substrate, taken to be predominantly W(110).

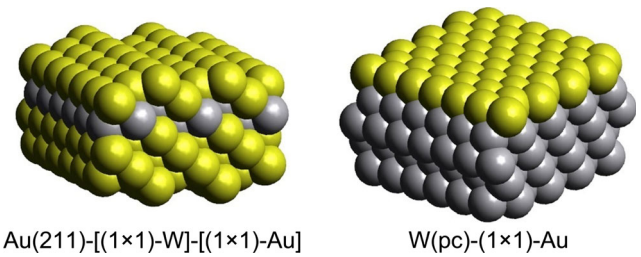

Fig. 1 Schematic illustration of the idealized structures of the Au(211)-[(1×1)-W]-[(1×1)-Au] and W(pc)-(1×1)-Au near-surface alloys

All electrodeposition experiments were performed with an SP-200 Bio-Logic potentiostat (Bio-Logic Science Instruments, Claix, France) in a three-electrode configuration. The freshly prepared near-surface alloy electrodes were rinsed with Nanopure water and immediately used for DEMS experiments.

Differential Electrochemical Mass Spectrometry

The principles of DEMS and its applications to electrochemical surface science have been amply discussed and reviewed [17–20]. A custom-made polyether ether ketone (PEEK) cell similar to the device described previously [21] was employed for the DEMS experiments. A 20-nm-porous 20-μm-thick polydimethylsiloxane (PDMS) membrane, hydrophobic in its unmodified state, separated the electrochemical cell from the mass spectrometry compartment. The disk-shaped working electrode with a geometric surface area of 0.90 cm^2 was separated from the PDMS membrane by a 50-μm glass spacer; such configuration resulted in a thin-layer electrochemical cell with a volume of 5.0 μL. A porous glass frit was placed between the working and the counter electrodes to prevent oxidation of the reduced products at the working electrode.

Controlled-potential measurements were carried out with a Bio-Logic SP-300 potentiostat (Bio-Logic Science Instruments, Claix, France) with electrochemical impedance spectroscopy capability to determine the uncompensated solution resistance (R_u); 85 % of R_u was compensated by the potentiostat.

The NSA electrode was placed in the DEMS cell containing a 0.1 M solution of 99.9 %-pure $KHCO_3$ (J. T. Baker, Center Valley, PA) purged with high-purity (99.99 %) CO_2 (Air Liquide, Plumsteadville, PA). For the CO_2 reduction, the potential was held at −1.8 V vs. Ag/AgCl (1 M KCl) reference[1] (CH Instruments) for 900 s while the reaction products were monitored by mass spectrometry; a Pt wire (Goodfellow, Coraopolis, PA) served as the counter electrode. Product detection was achieved via an HPR-20 quadrupole mass spectrometer (Hiden Analytical, Warrington, England) with a secondary electron multiplier detector operated at a voltage of 950 V and emission current of 50 μA.

In this *Letter*, DEMS results are described in terms of plots of *internally normalized* ion currents of the reduction products generated at a fixed potential as a function of time. Internal normalization is an established scheme in analytical chemistry to infer the *relative* amounts of analytes in a multicomponent mixture [22]. Selectivity was assessed by comparison of the relative amounts of *hydrogenated* products. The normalized ion current $[\mathrm{NIC}(t)_P]$ for a given product (P), such as methanol, at a given time (t) was obtained from:

$$\mathrm{NIC}(t)_P = {}^{\mathrm{IC}(t)_P}/_{\mathrm{IC}(t)_{P,W}} \quad (1)$$

where the subscript W indicates pure W. As an example, at 650 s, the IC signal at m/z=15 (methane) from W(pc)-(1×1)-Au was 6.6×10^{-17} A, whereas that from pure W was 6.9×10^{-17} A. Hence, under these conditions, the signals for methane from the NSA and from W were not distinguishable from one another: the computed NIC was 0.96. In other words, no methane was produced. For methanol, the IC signals at 800 s from W(pc)-(1×1)-Au and from W were, respectively, 2.3×10^{-17} and 0.58×10^{-17} A, to give an NIC value of 4.0; clearly, an appreciable amount of methanol was generated from the NSA.

The *absolute* quantities of products were determined via external calibration. The concentration of methanol, the lone CO_2-reduction product, was extracted from a plot of its IC as a function of the concentration of reference solutions. When that amount of methanol is used in Faraday's Law, the electrolytic charge for only the CO_2-to-CH_3OH reduction can be calculated. The ratio of such charge to the *total* charge empirically measured for the duration of the constant-potential electrolysis yields the current or Faradaic efficiency of the methanol-production reaction.

[1] Conversion between the pH-independent Ag/AgCl (1 *M* KCl) reference and the pH-dependent reversible hydrogen electrode (RHE) scale is given by: $E_{\mathrm{RHE}}=E_{\mathrm{Ag/AgCl\ (1\ M\ KCl)}}+0.197+(0.059\times\mathrm{pH})$. In this study, the pH after CO_2 saturation was 6.8; hence, −1.8 V [Ag/AgCl (1 M KCl)] corresponds to −1.2 V (RHE).

Results and Discussion

The thrust of the present study was towards the electrochemical reduction of CO_2 selectively to methanol at a W(pc)-(1×1)-Au near-surface alloy, as a qualitative test of predictions rendered by DFT simulations [9]. CH_3OH-product selectivity was evaluated by comparison of the amount of methanol formed with the quantities of three other hydrogenous fuels: methane, ethylene, and ethanol. The methodology involved the application of a fixed negative potential at the NSA electrode in a 0.1 M solution of HCO_3^- saturated with CO_2 gas from a 1-atm source, while the mass spectrum ion currents (MS IC) were monitored, as a function of time, for H_2 (m/z=2), CH_4 (m/z=15), C_2H_4 (m/z=26), CH_3OH (m/z=31), and CH_3CH_2OH (m/z=31, 45, and 46). With regard to the alcohols, the presence of a peak at m/z 31 but not at 45 and 46 would indicate CH_3OH, but no CH_3CH_2OH [23]. The potential applied was −1.8 V (Ag/AgCl) or −1.2 V (RHE), a voltage at which all possible CO_2-reduction products would have already been initiated [6]; at more negative potentials, the evolution of hydrogen gas overwhelms the DEMS cell. The NSA electrodes studied were of the overlayer type: n monolayers of gold on polycrystalline tungsten, W(pc)-n[(1×1)-Au], with n at 0.5, 1, 2, and 3 ML.

The electrocatalysis of CO_2 reduction is governed primarily by surface composition and secondarily by interfacial structure. With respect to composition, coulometric measurements based on Faraday's Law have indicated the formation of discrete numbers (0.5, 1, 2, or 3) of monolayers of Au on a W host substrate. The presence of the Au overlayers has been confirmed by X-ray photoelectron spectroscopy, although the spectra are not displayed here. Quantification based on XPS is not necessary since coverages have already been determined by coulometry, and it is Faraday's Law that calibrates XPS intensities, not the other way around. With regard to the structural nature of the Au overlayers, results from UHV-based studies of Au on W(110) [24, 25] have shown that submonolayer patches of Au evolve into a first monolayer that completely covers the surface; further addition of Au gives rise to three-dimensional growth.

The *normalized* ion currents, averaged from replicate measurements, of CH_4, C_2H_4, and CH_3OH as a function of time, are shown in Fig. 2; no plot is shown for ethanol since preparatory experiments indicated its absence in the product distribution. It needs to be pointed out that appreciably large bubbles from the H_2-evolution reaction sporadically altered the quantity of solution that contacted the membrane; as a consequence, the amount of product that passed through the membrane was also affected. It is the reason that the time dependence of the ion currents showed fluctuations over the 900-s spectral acquisition period. To minimize the non-systematic variations, only the highest value of the IC from multiple trials was used: the hydrogen bubbles only cause a decrease, not an increase, of the MS signals.

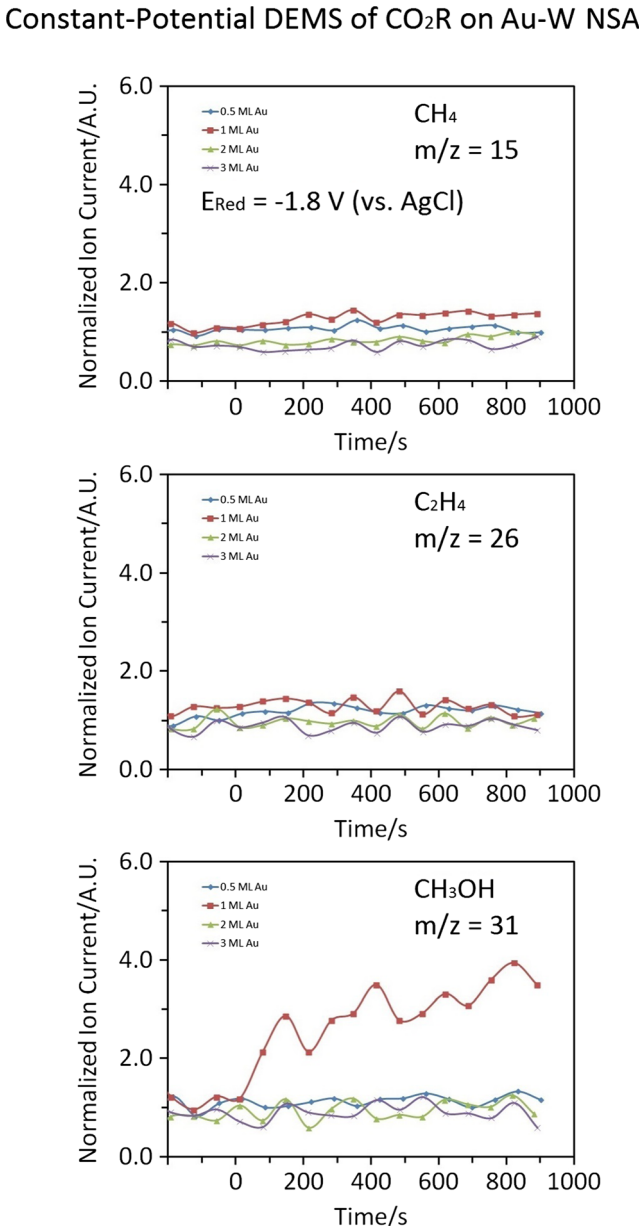

Fig. 2 Plots of *normalized* ion current as a function of time for CH_4 (*m/z*=15), C_2H_4 (*m/z*=26), and CH_3OH (*m/z*=31) generated from the constant-potential cathodic electrolysis, at −1.8 V (Ag/AgCl), of a CO_2-saturated 0.1 M $KHCO_3$ solution at W(pc)-*n*[(1×1)-Au], where *n* is the number of Au monolayers

The data for pure W and those for the 0.5-ML NSA electrodes do not diverge from one another. No enhancement in the catalysis was thus indicated from the submonolayer adlattices. It is also immediately obvious from the data in Fig. 2 that the normalized ion currents for CH_4 and C_2H_4 stayed essentially the same, equal to unity, regardless of Au coverage or electrolysis time. This can only signify that, with respect to methane and ethylene, neither catalytic activity nor product selectivity occurred; formation of the hydrocarbons would have resulted in a discernible upward slope of the IC-vs-t plots.

On the other hand, a stark contrast is advanced by the results shown in the bottom frame of Fig. 2: For W(pc)-(1×1)-Au, in which only one monolayer of Au exists, there is a prompt increase in the methanol MS signal as soon as the reduction potential is applied; there is also an obvious accumulation of the total ion current at the end of the acquisition period. The DEMS data thus serve as evidence for the *exclusive selectivity* of CH_3OH as a CO_2-reduction product, over CH_4, C_2H_4, or CH_3CH_2OH, at the W(pc)-(1×1)-Au NSA electrode. Interestingly, because it was not treated in the theory, both the activity and the selectivity decreased to zero when the Au coverage deviated significantly from 1 ML, such as when *n* was 0.5, 2, or 3.

The CH_3OH concentration at the end of the potentiostatic DEMS experiment was determined by external calibration to be 3 mM. That corresponds to a CH_3OH-product-exclusive activity of 52 μA cm^{-2} or a Faradaic efficiency of at least 0.50 %. A major fraction of the current was obviously consumed towards H_2 evolution and, given that the topmost layer was Au, probably also in the production of CO and formates that cannot be distinguished by DEMS. In comparison, with polycrystalline Cu, an earlier seminal study indicated no production of CH_3OH [1, 4], although a more recent study [6] has reported a current efficiency of 0.15 %, significantly lower than that for W(pc)-(1×1)-Au. No CH_3OH was detectable here at potentials less negative than −1.8 V. Hence, for the production of methanol, there may be only little or no improvement in the overvoltage. Regardless, it is clear that the suggested proclivity of W(pc)-(1×1)-Au towards selective methanol production has been (qualitatively) confirmed.

Limitations remain that point towards further study: the low catalytic activity, the large overpotential, and the non-suppression of the hydrogen-evolution reaction. The divergence between the computational prognoses and experimental diagnoses may be traceable in part to the fact that the polycrystalline W(pc)-(1×1)-Au overlayer alloy is not an adequate mimic of the sub-surface Au(211)-[(1×1)-W]-[(1×1)-Au] alloy, as prescribed in the theoretical work. Deficiencies in the theoretical treatment, to be presumed since all computational efforts are only approximations, may likewise be a factor but those are beyond the scope of the present investigation. Nevertheless, the empirical validation of the selective methanol production should provide sufficient impetus for expanded studies with a near-perfectly fabricated Au(211)-[(1×1)-W]-[(1×1)-Au] near-surface alloy.

Summary

The electrochemical reduction of CO_2 at Cu electrodes, while known to yield more than a dozen products, does not generate methanol. In this regard, a computational search was recently conducted for an electrocatalyst selective towards CH_3OH as

a product. The work, based upon density functional theory (DFT) and three adsorption-strength descriptors, $\Delta G°_{CO,ads}$, $\Delta G°_{OH,ads}$, and $\Delta G°_{H,ads}$, predicted the viability of a bimetallic NSA electrode made up of gold and tungsten. The present *Letter* describes results from an experimental study that tested the theoretical prediction via DEMS focused singularly on product selectivity towards methanol, away from methane, ethylene, or ethanol; the reduction of CO_2 was in a solution of 0.1 M $KHCO_3$ at −1.8 V (Ag/AgCl). At an overlayer NSA that consisted of *n* ML of Au on a polycrystalline W electrode, W(pc)-*n*[(1×1)-Au], no methane, ethylene, or ethanol was detected, when the coverage of Au was at submonolayer (n=0.5) or multilayer (n≥2) coverage. However, when the overlayer contained only 1 ML of Au, methanol was generated *exclusively*. The anticipated CH_3OH-product selectivity of the W(pc)-(1×1)-Au NSA has thus been (qualitatively) confirmed. The CH_3OH-selective activity was 52 μA cm^{-2} for a Faradaic efficiency of 0.50 %; the bulk of the current was expended towards H_2 evolution and, since the topmost layer was Au, most likely in the production of CO and formates that are undetectable by DEMS. The prognoses for heightened activity, decreased overpotential, and suppressed hydrogen evolution have not yet been substantiated and, along with a complete analysis of the product distribution, await further investigation. The mismatches may be traceable in part to the fact that the polycrystalline W(pc)-(1×1)-Au overlayer alloy investigated is not a suitable replica of the sub-surface alloy structure, Au(211)-[(1×1)-W]-[(1×1)-Au], as defined precisely in the theoretical work. Deficiencies in the computational treatment may also be a factor, but those are beyond the scope of the present pursuit. Nevertheless, the empirical validation of the selective methanol production provides sufficient impetus for expanded studies with a near-perfectly fabricated near-surface alloy.

Acknowledgments This material is based upon work performed by the Joint Center for Artificial Photosynthesis, a DOE Energy Innovation Hub, supported through the Office of Science of the U.S. Department of Energy under Award No. DE-SC0004993.

References

1. Y. Hori, in *Modern Aspects of Electrochemistry*, ed. by C.G. Vayenas, R.E. White, M.E. Gamboa-Aldeco (Springer, New York, 2008), p. 89
2. M. Gattrell, N. Gupta, A.J. Co, Electrochemical reduction of CO_2 to hydrocarbons to store renewable electrical energy and upgrade biogas. Energy Convers. Manage. **48**, 1255 (2007)
3. M. Gattrell, N. Gupta, A.J. Co, A review of the aqueous electrochemical reduction of CO_2 to hydrocarbons at copper. J. Electroanal. Chem. **594**, 1 (2006)
4. Y. Hori, A. Murata, R. Takahashi, Formation of hydrocarbons in the electrochemical reduction of carbon dioxide at a copper electrode in aqueous solution. J. Chem. Soc., Faraday Trans. 1, **85**, 2309 (1989)
5. J. Qiao, Y. Liu, F. Hong, J. Zhang, A review of catalysts for the electroreduction of carbon dioxide to produce low-carbon fuels. Chem. Soc. Rev. **43**, 631 (2014)
6. K.P. Kuhl, E.R. Cave, D.N. Abram, T.F. Jaramillo, New insights into the electrochemical reduction of carbon dioxide on metallic copper surfaces. Energy Environ. Sci. **5**, 7050 (2012)
7. A.A. Peterson, J.K. Nørskov, Activity descriptors for CO_2 electroreduction to methane on transition-metal catalysts. J. Phys. Chem. Lett. **3**, 251 (2012)
8. A.A. Peterson, F. Abild-Pedersen, F. Studt, J. Rossmeisl, J.K. Nørskov, How copper catalyzes the electroreduction of carbon dioxide into hydrocarbon fuels. Energy Environ. Sci. **3**, 1311 (2010)
9. S. Back, H. Kim, Y. Jung, Selective heterogeneous CO_2 electroreduction to methanol. ACS Catal. **5**, 965 (2015)
10. W.J. Durand, A.A. Peterson, F. Studt, F. Abild-Pedersen, J.K. Nørskov, Structure effects on the energetics of the electrochemical reduction of CO_2 by copper surfaces. Surf. Sci. **605**, 1354 (2011)
11. J.C. Slater, Atomic radii in crystals. J. Chem. Phys. **41**, 3199 (1964)
12. J. Greeley, M. Mavrikakis, Near-surface alloys for hydrogen fuel cell applications. Catal. Today **111**, 52 (2006)
13. A.S. Bandarenka, A.S. Varela, M. Karamad, F. Calle-Vallejo, L. Bech, F.J. Perez-Alonso, J. Rossmeisl, I.E. Stephens, I. Chorkendorf, Design of an active site towards optimal electrocatalysis: overlayers, surface alloys and near-surface alloys of Cu/Pt(111). Angew. Chem. Int. Ed. **51**, 11845 (2012)
14. A.S. Varela, C.G. Schlaup, Z.P. Jovanov, P. Malacrida, S. Horch, I.E.L. Stephens, I. Chorkendorff, CO_2 electroreduction on well-defined bimetallic surfaces: Cu overlayers on Pt(111) and Pt(211). J. Phys. Chem. C **117**, 20500 (2013)
15. M.C. Weidman, D.V. Esposito, I.J. Hsu, J.G. Chen, Electrochemical stability of tungsten and tungsten monocarbide (WC) over wide pH and potential ranges. J. Electrochem. Soc. **157**, F179 (2010)
16. C.G. Fink, F.L. Jones, The electrodeposition of tungsten from aqueous solutions. J. Electrochem. Soc. **59**, 461 (1931)
17. H. Baltruschat, in *Interfacial Electrochemistry*, ed. by A. Wieckowski (Marcel Dekker, New York, 1999), p. 577
18. H. Baltruschat, Differential electrochemical mass spectrometry. J. Am. Soc. Mass Spectrom. **15**, 1693 (2004)
19. Z. Jusys, H. Massong, H. Baltruschat, A new approach for simultaneous DEMS and EQCM: electro-oxidation of adsorbed CO on Pt and Pt-Ru. J. Electrochem. Soc. **146**, 1093 (1999)
20. T. Hartung, H. Baltruschat, Differential electrochemical mass spectrometry using smooth electrodes: adsorption and hydrogen/deuterium exchange reactions of benzene on platinum. Langmuir **6**, 953 (1990)
21. A. Javier, B. Chmielowiec, J. Sanabria-Chinchilla, Y.-G. Kim, J.H. Baricuatro, M.P. Soriaga, A DEMS study of the reduction of CO_2, CO, and HCHO pre-adsorbed on Cu electrodes: empirical inferences on the CO_2RR mechanism. Electrocatalysis **6**, 127 (2015)
22. D. Kealey, P.J. Haines, *Instant Notes in Analytical Chemistry* (Garland Science, New York, 2002)
23. S.E. Stein, Mass Spectra, in *NIST Chemistry WebBook, NIST Standard Reference Database Number 69*, ed. by P.J. Linstrom, W.G. Mallard (National Institute of Standards and Technology, Gaithersburg, 1990)
24. P.D. August, J.P. Jones, The epitaxy of gold on (110) tungsten studied by LEED. Surf. Sci. **64**, 713 (1977)
25. T. Giela, K. Freindl, N. Spiridis, J. Korecki, Au(111) films on W(110) studied by STM and LEED. Uniaxial reconstruction, dislocations and Ag nanostructures. Appl. Surf. Sci. **312**, 91 (2014)